TSINGHUA SCIENCE AND TECHNOLOGY
ISSN 1007-0214 05/13 pp 406–418
DOI: 10.26599 / TST.2018.9010034
Volume 23, Number 4, August 2018

An Efficient EH-WSN Energy Management Mechanism

Yang Zhang, Hong Gao*, Siyao Cheng, and Jianzhong Li

Abstract: An Energy-Harvesting Wireless Sensor Network (EH-WSN) depends on harvesting energy from the environment to prolong network lifetime. Subjected to limited energy in complex environments, an EH-WSN encounters difficulty when applied to real environments as the network efficiency is reduced. Existing EH-WSN studies are usually conducted in assumed conditions in which nodes are synchronized and the energy profile is knowable or calculable. In real environments, nodes may lose their synchronization due to lack of energy. Furthermore, energy harvesting is significantly affected by multiple factors, whereas the ideal hypothesis is difficult to achieve in reality. In this paper, we introduce a general Intermittent Energy-Aware (IEA) EH-WSN platform. For the first time, we adopted a double-stage capacitor structure to ensure node synchronization in situations without energy harvesting, and we used an integrator to achieve ultra-low power measurement. With regard to hardware and software, we provided an optimized energy management mechanism for intermittent functioning. This paper describes the overall design of the IEA platform, and elaborates the energy management mechanism from the aspects of energy management, energy measurement, and energy prediction. In addition, we achieved node synchronization in different time and energy environments, measured the energy in reality, and proposed the light weight energy calculation method based on measured solar energy. In real environments, experiments are performed to verify the high performance of IEA in terms of validity and reliability. The IEA platform is shown to have ultra-low power consumption and high accuracy for energy measurement and prediction.

Key words: energy harvesting WSN; energy efficiency; energy measurement; synchronous wakeup

1 Introduction

Wireless Sensor Network (WSN) has promising applications in structural monitoring, underwater detection, military, and radiology[1]. The WSN node senses environmental data, transfers data through muti-hop networks[2, 3], aggregates the data to the sink node[4, 5], and reconstructs the physical status by data process and analysis[6]. The key factor that restricts the application of WSN is energy. Although the sink node usually has sufficient power to meet a higher performance[7], the energy of sensing nodes is limited. The operation of WSN, including data aggregation, extraction, and query[8–10], considers energy efficiency, which motivates us to investigate methods of prolonging network lifetime as much as possible. A conventional WSN uses batteries to provide relatively sufficient energy for complex calculations and communications, whereas, its lifetime is limited. Once the battery is depleted, the WSN is paralyzed. In most practical application environments, replacing batteries is very inconvenient and even impossible, thereby reducing the practicability of WSN.

- Yang Zhang, Hong Gao, Siyao Cheng, and Jianzhong Li are with the Department of Computer Science and Technology, Harbin Institute of Technology, Harbin 150001, China. E-mail: zhang_yang@hlju.edu.cn; honggao@hit.edu.cn; csy@hit.edu.cn; lijzh@hit.edu.cn.
- Yang Zhang is also with the Department of Key Laboratory of Mechatronics, Heilongjiang University, Harbin 150080, China. E-mail: zhang_yang@hlju.edu.cn.
* To whom correspondence should be addressed.
Manuscript received: 2017-09-11; accepted: 2017-09-18

To prolong the network lifetime further, Energy-Harvesting (EH) technology is widely applied in WSN. EH-WSN is able to harvest environmental energy, such as light, Radio Frequency (RF), and wind energy, which are then converted into electrical energy and stored for WSN nodes. The energy of WSN is mainly stored in rechargeable batteries or capacitors. With high energy density, the rechargeable battery-powered WSN nodes have sufficient energy to operate in a manner similar to that of a traditional WSN as the networking protocol and algorithm are investigated sufficiently[11, 12]. The critical defect lies in the following: the charge cycle times are limited, and the rechargeable battery requires a large amount of energy for charging. Once the node loses power, it needs a long time to wake up or is even unable to restart, which leads to intolerable network delay and restricts the network lifetime seriously. A smaller capacitor only requires a small amount of energy to charge to a relatively high voltage, thereby achieving shorter network delay and almost unlimited lifetime compared with that of the traditional mechanism. Therefore, EH-WSN has to apply capacitors to store electrical energy. The energy supply structure of EH-WSN is shown in Fig. 1.

Subject to the cost and size of nodes, EH-WSN is only able to harvest limited energy. EH-WSN uses a capacitor within a range of approximately 10–2200 μF, which is 6–8 orders lower than that of the batteries used by traditional WSN nodes (such as TELOSB)[13]. The filled capacitor supports EH-WSN to perform a limited degree of computation and communication. Thus, EH-WSN must be an intermittent operation platform where nodes harvest energy continuously and wake up and perform computation and communication only when sufficient energy is available to complete necessary operations. Accordingly, EH-WSN has to solve the following problems:

(1) Node synchronization. Owing to the limited energy, EH-WSN is able to communicate for only a short time, and the nodes have to communicate in a synchronized time slot[14, 15]. EH-WSN usually runs out of power due to lack of energy and misses the time slot, thereby causing low efficiency of network communication or even paralysis. Nodes lose synchronization when the network is restarted and require additional energy to achieve synchronization.

(2) Intermittent operation. Owing to energy shortage, EH-WSN usually runs out of power before the computation or communication is finished, thereby causing failure and energy wastage. Thus, EH-WSN has to know the exact energy information to plan its operations and should be able to perform basic energy management functions to avoid unexpected power cuts.

The traditional WSN adopts batteries to supply power without the aforementioned problems. Nodes have sufficient energy to seek the global optimal solution for energy consumption and plan the network strategy[16, 17]. For EH-WSN, most of the existing algorithms assume that nodes are synchronized and the harvesting energy in each time slot is known[18–23]. However, the existing EH-WSN platform is unable to support its expected functions[11, 12, 24, 25]; therefore, most of the existing scheduling algorithms based on EH-WSN can calculate energy only by relying on energy models. In fact, the energy harvested and consumed is affected by variable factors; thus, the calculation based on energy models encounters a significant error that increases the node computation. The results of simulated experiments are significantly different from those of practical applications. Therefore, EH-WSN is urgently needed for a wireless sensor platform to provide accurate energy data and wakeup nodes on time during intermittent operation.

Based on the proceeding discussion, this paper proposes an Intermittent Energy-Aware (IEA) WSN platform, which achieves synchronization for intermittent running nodes in terms of hardware and software and also provides accurate energy data. The photo of this platform is shown in Fig. 2. This paper makes the following contributions:

(1) It presents the design of a practical EH-WSN platform that is complete and applicable in real environments. With the double-stage capacitor structure to store energy, IEA is able to continue working in poor energy environments. Furthermore, IEA provides support for intermittent synchronization and intermittent operation

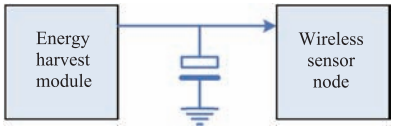

Fig. 1 Energy supply of EH-WSN.

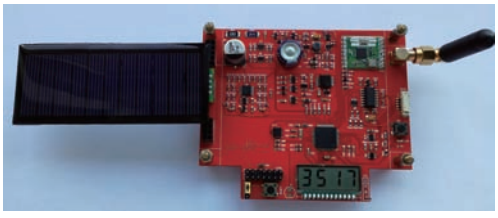

Fig. 2 Photo of IEA platform.

in terms of software and hardware. IEA achieves the function of auto power supply such that the quiescent current is less than 2 μA when powered up, whereas the quiescent current is less than 0.5 μA when powered down, ensuring high energy efficiency and preventing loss.

(2) In real environments, the accurate energy measurement with ultra-low power for EH-WSN is implemented for the first time. IEA measures power with a current sensing circuit and uses the analog integrator to accumulate the amount of charge that is harvested and consumed within a particular period. Then, the accurate measurement is realized and the CPU time is reduced significantly. Experiments show that the energy measured by IEA is extremely close to the real value with an average accuracy of 99.89%, and the energy cost is only 157 μW.

(3) According to the circuit model of solar panel and the charge characteristics of capacitance, this paper proposes a light-weight energy prediction method based on solar batteries, of which the average prediction error is only 0.74%.

The rest of this paper is organized as follows. Section 2 provides the background and summarizes related works. Section 3 describes the energy management implementation in detail. Section 4 evaluates the system. Finally, Section 5 provides a summary and final remarks.

2 Related Work

Similar to the traditional WSN network, EH-WSN also senses environmental data, transmits the data to the sink reliably through a specific network protocol, and restores the real-world physical information through data query and mining[26–28]. The difference lies in that EH-WSN has to consider the influence of energy. Existing EH-WSN research strategies usually assume that nodes are synchronized, and the harvested and consumed energy is known or predictable[20–23]. Ren et al.[23] utilized a representative energy module expressed as

$$B_v(t) = min(B_v(t-1) + Q_v(t-1) - S_v(t-1) - e,\ C_v) \tag{1}$$

where, C_v refers to the energy stored in the capacitor; $B_v(t)$ is the stored energy at t moment; $Q_v(t)$ and $S_v(t)$ are the harvested and consumed energy at t moment, respectively; e refers to the circuit consumption. Nodes need accurate $B_v(T)$, $Q_v(T)$, $S_v(T)$, and C_v to plan network communication[20, 21]. Previous studies recognized that the harvesting energy can be estimated from historical data, and the energy consumed can be calculated according to the length of communication. Since the capacitance is known, the available energy is calculated. In practice, however, the estimated energy is far from the real value. First, the charge rate of the capacitor is nonlinear, and the actual rate depends on the initial voltage, source voltage, and capacitance. Furthermore, the charging rate drops sharply as the voltage of capacitor increases. Second, when the node of EH-WSN works, the capacitor voltage fluctuates with the specific operation, so the harvesting energy depends not only on the external environment but also on the state of the node itself. Finally, the capacitance is not highly accurate, because it is affected by environmental temperature and voltage, and the error of the capacitor value is up to 50%. Therefore, based on the labeled capacitor value, the maximum power and existing power of the capacitor, which are calculated, are not reliable. This model cannot support EH-WSN operation in a real environment; thus, EH-WSN requires true and reliable energy data to ensure stable operation.

The existing EH-WSN platforms are incapable of providing various types of energy data. The traditional WSN can determine the energy state by measuring the battery voltage. For EH-WSN with a capacitor, most of the platforms can calculate the stored energy by $E = CV^2/2$[13, 19, 24, 29]. However, the method can perceive only the current residual energy but not the specific harvested and consumed energy, while the capacitance offset of the capacitor seriously affects the accuracy of the calculated energy. Few of the existing EH-WSN platforms have energy measurement functions. The EnHANT nodes designed by Gorlatova et al.[12] adopt a current-sensing amplifier to amplify the current of the energy-harvesting circuit, whereas, the method by Gorlatova et al. is only able to measure the instantaneous value of the current. To sense the energy harvested for a particular period, the instantaneous current has to be sampled and summed up to calculate the total charge, thereby requiring a large amount of CPU time and energy, and interruptting the node operation seriously. Moreover, the discrete sampling leads to errors. Hassanalieragh et al.[25] proposed an energy-harvesting platform called UR-SolarCap with moderate-power systems based on solar energy. The platform uses a current-sensing amplifier circuit and collects discrete current value with a PIC controller to calculate energy; unfortunately, the energy consumption is only up to 10 mW, which is not applicable for EH-WSN.

In commercial platforms, some companies have launched development suites for harvesting nodes, such as Solar Dice by TI, CYALKIT-E03 (with solar energy)

by CYPRESS, and P2110-EVAL (with RF energy) by Powercast. In these commercial platforms, energy is stored in the capacitor for nodes to sense data and communicate via RF or blue-tooth. However, the nodes work only when the capacitor voltage exceeds the threshold, and the wakeup time is uncertain. Furthermore, these platforms obtain the capacitor voltage but not the specific energy profile. Therefore, the existing commercial EH-WSN platform is suitable only for single-hop star networks but is difficult to employ in the multi-hop topology structure. In fact, many existing EH-WSN studies and platforms have not yet considered intermittent operation. Thus far, no platform is capable of accurately measuring the energy with ultra-low power consumption, and no platform can wake up on time in the energy absence environment.

3 Implementation of Energy Management

EH-WSN has multiple energy harvesting sources such as solar, RF, thermoelectric, and wind energy. In this study, the IEA platform is not restricted to a specific energy-harvesting source but is available to various energy sources. The energy storage of EH-WSN mainly includes the rechargeable battery and capacitor. The capacity of the rechargeable battery is much larger than that of the capacitor. Although the rechargeable battery is able to ensure that nodes operate continuously with sufficient energy, the demanded power for charging is much larger than that for the capacitor. Once the node loses power due to lack of energy, restarting is difficulty. Thus, the rechargeable battery is not practical for extensive application because it does not conform to the original intention of EH-WSN. The capacitor proposed in this paper stores energy in a manner characterized by fast charging, minimal leakage, and low cost. The capacitor is able to charge to a relatively high voltage by using only a small amount of energy, thereby ensuring shorter wake-up periods for EH-WSN. Furthermore, the capacitor can boundlessly extend the network lifetime of EH-WSN due to its infinite charging cycles.

The IEA platform contains multiple modules and functions. This chapter mainly describes the energy management mechanism of the structure as shown in Fig. 3. The red lines represent energy flow, and the blue lines indicate data and signals. The energy obtained by the energy-harvesting module is directly stored in the electrolytic capacitor C_1, when the voltage reaches a threshold, the voltage-detection module starts to supply power and MicroController Unit (MCU) starts to work. The smaller the capacitor C_1 is, the higher the wake

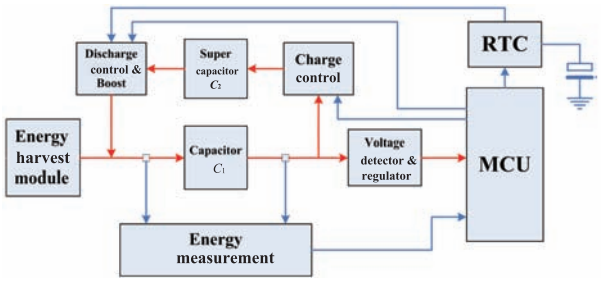

Fig. 3 Energy structure of the IEA platform.

frequency is, and the capacitance usually meets the lower bound of the demand. MCU can measure real-time energy data from the energy measurement module. When the capacitor C_1 is overfilled, MCU can trigger the charging circuit to charge the excess energy into the super capacitor C_2. Before nodes are powered-off due to insufficient energy, MCU can set the Real-Time Clock (RTC) to trigger the discharge circuit from C_2 on time to ensure that the nodes wake up synchronously even when energy is lacking.

3.1 Double-stage energy storage and synchronous wakeup

The energy, such as solar energy, obtained by EH-WSN is usually fluctuant. The energy reaches its peak value under direct sunlight in day-time, usually with more than the maximum capacitance of the capacitor, whereas in the evening, as the harvested energy is nearly zero, the nodes may have no power for a longtime, and this condition nearly leads to network paralysis. To ensure that nodes wake up periodically even with lack of energy, we have to store the excess energy in a super capacitor when the amount is sufficient. Therefore, we designed a double-stage capacitor structure for electrolytic and super capacitors. The harvested energy is stored directly in the electrolytic capacitor C_1, which has small capacitance, to ensure short wake-up periods of the nodes. The excess energy is stored in the super-capacitor C_2 for use when energy is lacking. The circuit structure is presented in Fig. 4.

The charging and discharging circuit for the super capacitor is in the frame marked by red dots. Since the capacitance of C_2 is much larger than that of C_1, if C_1 connects to C_2 directly, C_2 will suck the voltage of C_1 in an instant, thereby causing the nodes to power down. Therefore, MCU needs to output a Pulse Frequency Modulation (PFM) signal to trigger the Metal-Oxide-Semiconductor Field-Effect Transistor (MOSFET) Q_3 and control the charging current into C_2. This method is easy to apply with low cost, whereas MCU is needed to monitor the C_1 voltage in real time and prevents this voltage from

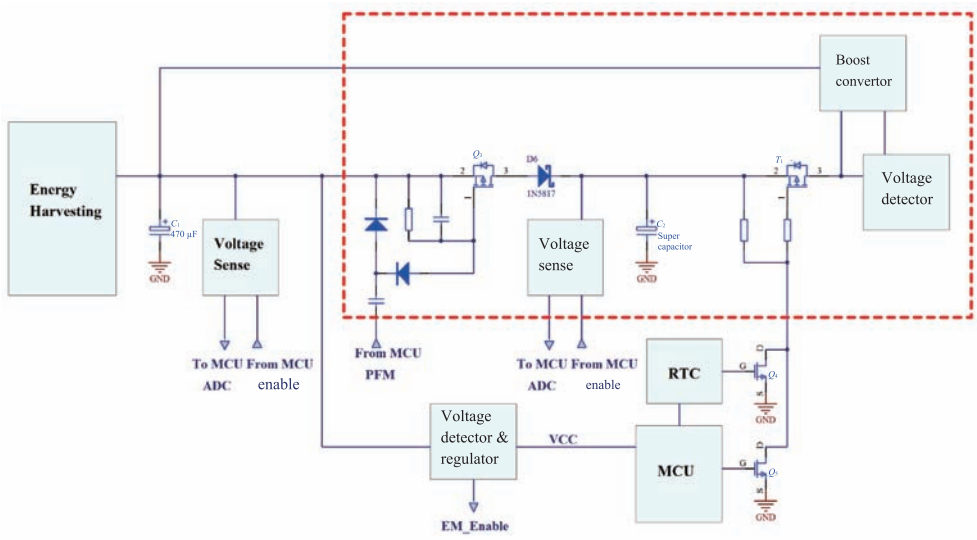

Fig. 4 Double-stage capacitor energy management structure.

dropping too low and causing power failure.

When the energy is insufficient, MCU or RTC can control T_1 to discharge C_2. Two common situations may occur: (1) When MCU performs the key computation or communication and C_1 voltage is not enough to complete the operation, MCU controls C_2 to discharge to complete the key operation. (2) When C_1 can not reach the working voltage, the RTC module controls C_2 to discharge based on a synchronous clock to start the system. Owing to the large capacitance of the super capacitor, a large amount of current is needed to charge C_2 to a relatively high voltage. Therefore, using the BOOST converter to lift the discharge voltage is necessary. As the conversion efficiency of the BOOST converter can not reach 100%, IEA uses a voltage detector. Only when the C_2 voltage is below 2.7 V, the BOOST converter can start to work and the output voltage is stabilized at 3 V. Notably, T_1 must be a low drain-source on-resistance MOSFET to ensure that C_2 discharges fully at low voltage.

In addition, we designed the voltage detection and regulator circuit as shown in Fig. 4. The circuit starts to supply power only when the C_1 voltage exceeds 2.1 V. When the C_1 voltage is below 2.0 V, the power supply switches off to avoid wasting energy because the chips are powered insufficiently and may consume an abnormal amount of energy[30]. Furthermore, the RTC module holds the synchronous clock by relying on the internal capacitor, so the module has to wake up the nodes before the capacitor voltage is less than 1.1 V, which prevents the loss of synchronization.

The capacitance of C_1 demands careful consideration. If C_1 is extremely small, the nodes may not have sufficient energy to run large tasks, whereas if C_1 is extremely large, the response frequency of nodes is reduced and energy is wasted. IEA is preset to send 3 packets of 10 bytes and receive 100 ms of data when it is charged to 2.7 V. The RF chip should work under constant voltage of 2.1 V with transmission power of 1 dbm (at 25 Kbps), while the sending current is approximately 14.1 mA, the duration of a 10-byte packet is approximately 6.6 ms, and 3 packets of energy are approximately 587 μJ. Meanwhile, the receiving current is 3.3 mA, so the energy of 100 ms is approximately 693 μJ. Therefore, the capacitor C_1 must have the capacitance to store at least 1280 μJ of energy. According to $E = CV^2/2$, as the energy is stored in the capacitor, the capacitor C_1 with the value of 1000 μF meets the requirement.

3.2 Energy measurement with ultra low power consumption

The most direct and reliable way to obtain the real energy data is to take actual measurements. In Fig. 5, the energy for nodes is stored in C_1; thus, the harvested and consumed energy is the energy that flows into and out of C_1, respectively. As the measurement circuits of energy harvesting and energy consumption are identical, we take the energy harvesting measurement as an example to describe in detail. The harvested energy can be calculated by $E = \int_0^T U(t)I(t)\mathrm{d}t$. According to the equation, knowing the value of voltage and current within T time is necessary. As the voltage of C_1 varies minimally over a short period of time, $U(t)$ can be approximated by the

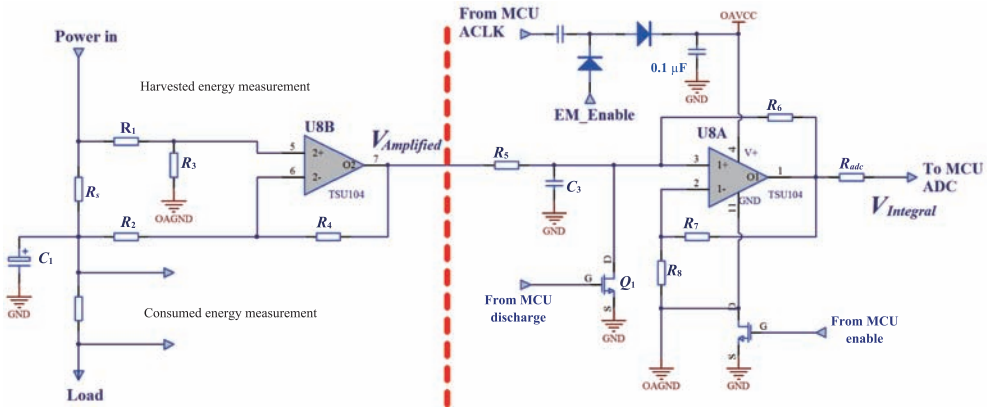

Fig. 5 Energy measurement circuit.

average value, and then the harvested energy can be calculated as the value of $\int_0^T I(t)\mathrm{d}t$. The key problems are how to amplify the weak current signal for MCU measurement; and how to reduce the energy consumption for the measurement. The existing platform has used the current sensing circuit and sampled a set of discrete current values to obtain the total charge by adding the proceeding current values, which requires a large amount of CPU time and energy and seriously interrupts the normal operation of nodes. Moreover, the discrete samplings may produce sampling errors that affect the accuracy.

To measure $\int_0^T I(t)\mathrm{d}t$ with the lowest energy and solve the problem, we used the high-side current sense amplifier and integrated circuit. The circuit in Fig. 5 includes two sections, where the left section is the current sense and amplifier circuit, and the right section is the integral circuit. When current flows through the sense resistor R_s on the left side, it produces a slight voltage drop of $V_{Rs} = I_{Rs} \cdot R_{Rs}$, which is amplified by the first-stage amplifier $U8$-B with output of V_{Amp}. To simplify the calculation, we suppose that $R_1 = R_2$, $R_3 = R_4$ to obtain the output value $V_{Amp} = \dfrac{R_3}{R_1} V_{Rs}$, which is placed in the integral circuit of the right side. To simplify the calculation, we suppose that $R_5 = R_6$, $R_7 = R_8$, and then the output value V_{Integ} to MCU is as shown in Eq. (2):

$$V_{Integ} = \frac{2}{R_5 C_3} \int V_{Amp}(t)\mathrm{d}t = \frac{2R_3 R_{Rs}}{R_5 C_3 R_1} \int I_{Rs}(t)\mathrm{d}t \quad (2)$$

We suppose that the average voltage of capacitor C_1 at t time refers to $V_{c1}(t)$, and then the harvested energy $E_{harv}(t)$ at t second is calculated in Eq. (3) as follows:

$$E_{harv}(t) = \int_{t-1}^{t} U(t)I(t)\mathrm{d}t =$$

$$\frac{V_c(t)+V_c(t-1)}{2} \int_{t-1}^{t} I_{Rs}(t)\mathrm{d}t =$$

$$\frac{R_3 R_{Rs}}{R_1 R_5 C_3} \cdot V_{Integ} \cdot (V_{c1}(t)+V_{c1}(t-1)) \quad (3)$$

Once the resistance is determined, MCU is only demanded to measure $V_{c1}(t)$ and V_{Integ} once per second and performs simple multiplication to obtain the harvested energy (J) in one second, which significantly reduces the calculation and wake-up time, thereby decreasing the power consumption. In fact, the integral output value V_{Integ} represents the electric charge obtained in this second. As measured once, the MOSFET Q_1 is responsible for discharging the capacitor C_3 to reset the measurement value.

In actual application, setting an appropriate RC value according to the range and accuracy is necessary. First, we should ensure that the input offset voltage of the operational amplifier is amplified with the amplification of R_3/R_1, thereby resulting in a significant measurement error. Generally, the lower the power consumption of an operational amplifier is, the higher the offset voltage becomes, so amplification has to be reduced. Second, when the current flows through the sampling resistor R_s, the voltage drop affects the stability of the supply voltage; thus, the R_s value needs to consider both the amplification and voltage stability. Finally, the value of $R_5 C_3$ in the integral circuit refers to the integral coefficient, and the value depends on the sampling interval and output voltage range. The aforementioned resistors need 0.1% precision components. As the capacitance error is relatively large, we recommend using an LCR meter to determine its specific value. All of the RC values determine the range and accuracy of measurements.

As shown in Fig. 5, we adopted a charge pump for the power supply of the operational amplifier to ensure that the

common mode input voltage is within the operating range. In addition, the resistor R_{adc} is responsible for reducing the leakage current when nodes sleep, whereas the larger resistor R_{adc} requires longer Analog-to-Digital Convertor (ADC) sampling time.

3.3 Solar energy-harvesting prediction

To plan network strategy in EH-WSN, predicting the harvesting energy in the next period of time is necessary. Moreover, different from traditional WSN networks, EH-WSN requires a higher precision of energy data, while only a small amount of energy is available for the prediction. In this section, we take the solar battery as an example of an energy source to describe in detail. We consider the overall solar battery characteristics, the offset of capacitance, and the charging curve to propose a solar energy prediction method based on the IEA platform. Note that the Maximum Power Point Tracking (MPPT) method is not applied here, and the solar batteries are directly connected to IEA. The charging curve of the capacitor is shown in Fig. 6, and the variation of voltage with time is shown in Eq. (4):

$$V(t)=V(0)+(V_{in}-V(0))\cdot(1-\mathrm{e}^{(-\frac{t}{RC})}) \tag{4}$$

Wherein, $V(t)$ refers to the charging voltage at t time, $V(0)$ is the initial voltage of capacitor, V_{in} is the supply voltage, and R and C are the resistance and capacitance values, respectively. The charging rate is nonlinear. When the initial voltage is close to zero, the voltage rises with the fastest speed. As the voltage rises, the charging current tends to zero, so it needs almost unlimited time to fill the capacitor. In fact, filling the capacitor is not necessary for EH-WSN to operate. What is important is to reach a voltage that is enough for operation and prediction. We strike a balance between the task load and the wake-up frequency.

(1) Once it wakes up, EH-WSN needs to perform actions of sensing, computation, and communication with enough energy stored in the capacitor. Based on the assumption that the operating voltage is 2–3 V, the current is approximately 1–20 mA, and the duration is approximately 10–100 ms, the energy required is 20–6000 μJ. According to the calculation of E=$CV^2/2$, the capacitance value range is 8–2400 μF. In this range, we can only utilize an electrolytic capacitor with an error of 10%–50% itself. Therefore, the actual capacitance of the capacitor should be confirmed before the node energy is calculated.

(2) The voltage of the capacitor is affected by the running action of nodes, such as the amount of calculation and communication, the number of resending, and so on. In a unit time, the lower the initial voltage of capacitor is, the more the energy flows into the capacitor. We have to consider that the capacitor voltage is affected by the action of nodes when calculating and predicting the energy.

(3) Subjected to the limitation of cost and size of EH-WSN, the existing environmental energy source is almost equivalent to a high resistance voltage source, and the output voltage varies with the current. The real source voltage V_{in} and the internal resistance R is unknown, which actually affects the energy-harvesting efficiency. Although the capacitance has an Equivalent Series Resistance (ESR), its resistance is negligible compared with the internal resistance of the energy source.

To predict the harvesting energy from solar batteries, the equivalent circuit of solar batteries is taken as a reference, as shown in Fig. 7. As the diode in the circuit is a nonlinear component with unknown parameters, calculating the energy is difficult. In fact, the light from solar panels varies minimally in a short period (a few seconds). Therefore, the left section of the equivalent model of solar batteries can be considered as a constant voltage source, and the circuit of the energy harvesting section of IEA is shown in Fig. 8. It is also an equivalent circuit for many energy components, such as thermoelectric[31]. From $t-1$ to t time, the amount of obtained charge is $Q_{harv}(t)$, and the amount of consumed charge is $Q_{csum}(t)$. As the average harvested current is $I_{harv}(t)=Q_{harv}(t)$ from $t-1$ to t, the average consumed

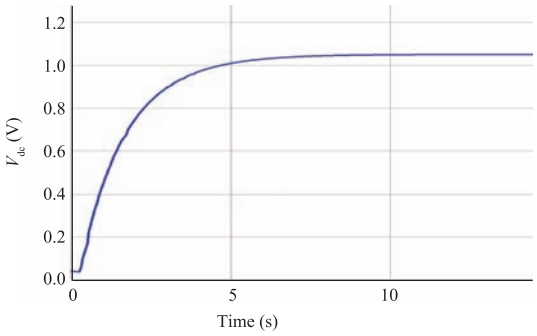

Fig. 6 Charging curve of the capacitor.

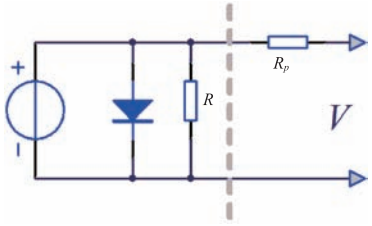

Fig. 7 Equivalent circuit of solar batteries.

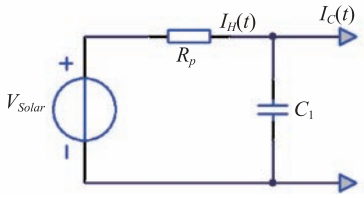

Fig. 8 Equivalent energy harvesting circuit of IEA.

current is $I_{csum}(t) = Q_{csum}(t)$. The known parameters are used to calculate the energy source voltage V_{Solar}, internal resistor R_p, and capacitance C_1.

On account of energy data measured by previous energy measurement circuits, the calculation of the three unknown parameters in the IEA platform is simple. In Fig. 8, as the increment of voltage and charge is known, the true value of the capacitor can be calculated directly according to $C_1 = \triangle Q / \triangle U = (Q_{harv}(t) - Q_{csum}(t))/(V_{c1}(t) - V_{c1}(t-1))$, and then we continuously measure the current $I_{harv}(t)$ and the capacitor voltage $V_{c1}(t)$ three times. According to $V_{Solar} = I_{harv}(t) \cdot R_p + \frac{(V_{c1}(t) + V_{c1}(t-1))}{2}$, the energy source voltage V_{Solar} and internal resistor R_p can be calculated.

In actual environments, since the measured voltage and charges have errors, the energy source voltage V_{Solar}, internal resistance R_p, and capacitance C_1 calculated by a single measurement are not so accurate. On the other hand, these physical parameters may vary with time. To improve energy prediction accuracy, we utilized Exponentially Weighted Moving-Average (EWMA) algorithm[23] to smooth the value, as shown in Eq. (5).

$$\overline{C_1}(t) = w \cdot \overline{C_1}(t-1) + (1-w) \cdot C_1(t) \tag{5}$$

In the equation, $C_1(t)$ is the measured capacitance value of t time, $\overline{C_1}(t)$ refers to the average capacitance value after weighting, w is the weight, and $0 < w < 1$. We select an appropriate w value to ensure a balance between the stability and response speed of changes. In the smoothing method, the energy source voltage V_{Solar} and internal resistance R_p are processed in the same principle.

Since the energy consumption of the hardware is known, EH-WSN nodes can predict the consuming energy based on the expected operation, such as Eq. (6).

$$E_{csum} = P_C t_C + P_T t_{TX} + P_R t_{RX} \tag{6}$$

E_{csum} refers to the consuming energy as predicted; P_C, P_T, and P_R refer to the power of computing, sending, and receiving, respectively; and t_C, t_{TX}, and t_{RX} refer to the expected time for computing, sending, and receiving, respectively. Once the EH-WSN nodes wake up, they execute necessary operations within a short time. Most of the time, however, the nodes stay asleep and t_C, t_{TX}, and t_{RX} can be neglected in energy calculation. According to $E = \frac{CV^2}{2}$, nodes consume the energy of E_{csum}, and then the C_1 voltage drops to $\sqrt{V_{c1}^2(0) - \frac{2E_{csum}}{\overline{C_1}}}$. According to Eq. (7), the energy E_{harv} can be estimated in the future t time, or the time t can be estimated by the specified energy E_{harv}. Thus, to harvest a large amount of energy, the stored energy in the nodes has to be consumed to reduce $V_{c1}(0)$ and the appropriate charging time t has to be selected.

$$E_{harv}(t) = \frac{\overline{C_1}}{2}\left(\overline{V_{Solar}} - \sqrt{V_{c1}^2(0) - \frac{2E_{csum}}{\overline{C_1}}}\right)^2 \cdot \left(1 - \mathrm{e}^{(-\frac{2t}{R_p \cdot C_1})}\right) \tag{7}$$

4 Experiments

In this section, the IEA platform is evaluated from four aspects: power consumption, energy management, measurement, and prediction. First, the experiment setting is introduced.

The IEA platform prototype uses an MSP430FR6972 micro-controller with an ultra-low-power consumption and takes a nonvolatile Ferromagnetic Random Access Memory (FRAM) with 64 KB. In the experiments, IEA did not adopt the operating system, but it optimized the source code to minimize the power consumption to the most extent. The parameters of the prototype are set as follows: the voltage range is 0–6 V; the node starts automatically when the voltage is higher than 2.36 V and powers down when the voltage is less than 2.0 V. MCU is powered by Low Dropout regulator (LDO) and works stably at 2.1 V. Capacitor C_1 has a capacitance of 1000 μF with ESR as 80 mΩ, and super capacitor C_2 has a capacitance of 0.1 F with ESR as 200 Ω. In energy measurement, IEA uses the operational amplifier (type TSV714), of which the consumption current is 9 μA/channel under 3 V supply, the input offset voltage is 0.2 mV, and the gain bandwidth is 120 kHz. Sensors mainly include light, temperature, and acceleration sensors (type ADXL327). The RF chip is SX1211 with communication frequency of 868 MHz, bit rate of 25 Kbps, and antenna gain of 2.5 dBi. All components are Commercial Off-the-Shelf (COTS), and consider performance and cost. The instruments used in the experiments are an oscilloscope Keysight MSOX3024A, a digital multimeter Keysight

34461A, a signal generator Rigol DG4102, and an illuminance meter UNI-T UT381.

4.1 Running energy consumption test of IEA

As an energy-harvesting platform, IEA itself must have low enough consumption to save more energy for computation and communication. In this section, we measured the power consumption of the IEA platform in sleep, standby, computation, and communication modes, and then conducted a running test of IEA.

(1) Power consumption in sleep mode

Sleep mode is the situation when the voltage of capacitor C_1 is below 2 V. At this point, the chip is unable to work and IEA is powered down automatically. Figure 9 shows the current variation in which IEA consumes itself when the voltage increases from 0–3 V in 30 s. To ensure that the measurement result is not affected by the charging capacitor, we did not add the capacitor C_1. IEA is set to sleep mode after booting without further computation and communication. As shown in Fig. 9, when the voltage is lower than 2.36 V, the average current consumption of IEA is 0.496 μA; when the voltage reaches 2.36 V, the consumption is approximately 3.7 mA in 16 ms. IEA produces the peak current of 3.7 mA due to power up and charging the internal capacitors, and then the current drops to 21 μA. After flowing 216 ms from the peak, the MCU starts to initialize with the duration of 153 ms and average current of 347 μA. Then, the node goes to sleep mode with the current of 3.46 μA. In fact, when the voltage is constant at 1.8 V, the sleep current of IEA is less than 1 μA, which is only approximately 1/20 compared with the current of the most power-saving Wireless Identification and Sensing Platform (WISP) nodes on the existing platforms.

(2) Power consumption in running mode

Operation mode is the situation when the voltage of capacitor C_1 is higher than 2 V. At this point, IEA is powered and capable to perform the computation and communication tasks. Figure 10 shows the current variations of IEA at the constant voltage of 2.5 V at the action of sleep, computation, and communication.

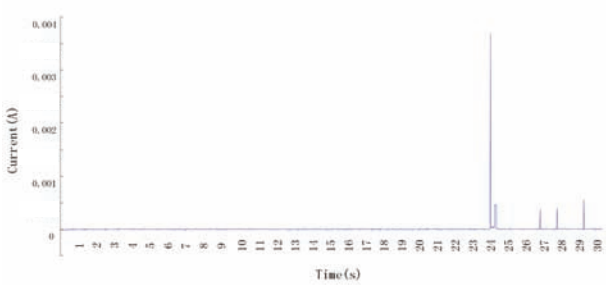

Fig. 9 IEA booting power consumption.

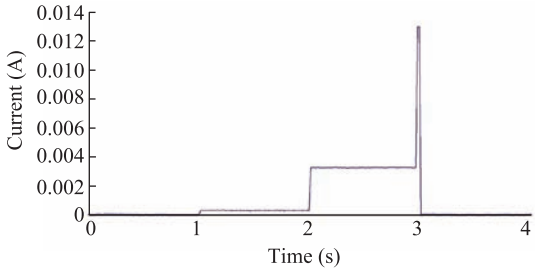

Fig. 10 IEA current in different modes.

First, IEA is in sleep mode with the current consumption of 48.9 μA mainly for the energy measurement module. After 1 s, MCU wakes up and computes with the current consumption of 333 μA. At 3 s, IEA comes into the receiving state with the current consumption of 3.284 mA. At 4 s, IEA sends three data packets with sending power of −8 dBm, 10 bytes per packet, and consumption current of 12.9 mA. After sending, MCU goes to sleep with the current of 48 μA.

(3) IEA running test

This section tests the energy-harvesting efficiency of the IEA platform under different illumination conditions including direct sunlight, cloudy day, and indoor lamp. IEA wakes up every second and measures energy. If it detects that the voltage exceeds 2.5 V, it sends a data packet of 10 bytes with the power of −8 dBm. At midday, when the sun is shining directly, IEA can send a packet every second with the voltage remaining at approximately 5.8 V. In fact, in direct sunlight, IEA nodes are free to compute and communicate without considering the energy limitation. In cloudy days, by the window, IEA can send a packet every second with illuminance of 2000 lx, and the voltage is maintained at approximately 4.2 V. At night, under lamp-light (LED), the IEA communication cycle is 3 s, and the voltage variations of nodes are shown in Fig. 11.

4.2 Energy storage and synchronous wake-up test

The IEA platform is able to continue working in an environment with lack of energy. In the experiments, the node was placed beside the window to monitor the variation of light in an entire day. The node was

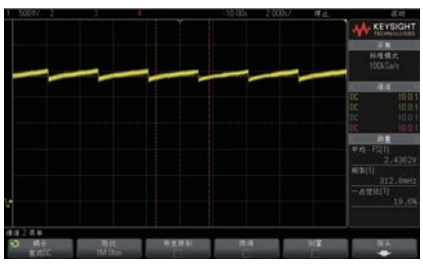

Fig. 11 Variation of IEA voltage.

synchronous with the sink every minute and needed time to initialize. Therefore, RTC had to wake up the node one second before synchronization to measure the current illumination, and then transmit data in synchronous time. The test was conducted from 9:00 am to 9:00 am of the following day. The experimental data are shown in Fig. 12.

As observed, from 7:00 pm to 9:00 pm, the intensity of illumination rises in the light of the fluorescent lamp; after 9:00 pm, the intensity of illumination stays in low position as the light is switched off. As early as 4:00 am, the light gradually intensifies because of sunrise. For 24 hours, the maximum voltage value of capacitor C_2 is 5.77 V, the minimum value is 3.34 V, and the transmission success rate is 98.3% in the time window of 60 ms. We can observe that the IEA platform can meet the communication requirements of the network in an environment where no energy is harvested, such as at night. If more data are to be transferred, we can use a larger super capacitor that requires more energy.

4.3 Experiment for energy measurement

As the principle and structure of energy-harvesting measurement and energy consumption measurement are identical, we compared only the measured harvested energy with real values. IEA is powered by a solar battery and works 100 s continuously. The node wakes up per second to measure current energy, receive 50 ms of data, send a 10-byte data packet, and then falls asleep. In circuit, R_1=R_2=10 KΩ, R_3=R_4=R_5=R_6=R_7=R_8=2 MΩ, C_3=1 μF. The resistor R_s refers to 10 Ω in the energy measurement; based on the calculation of Eq. (3), when the sampling period is one second, the amplification factor is 1000, and the measuring range is 1 mA. Figures 13–15 show a comparison between the measured results and real values of the IEA platform. In Fig. 14, we can observe the comparison of the energy measurement between the IEA platform and the actual value, and also the measuring error for each time.

As shown in Fig. 13, the current measured by IEA

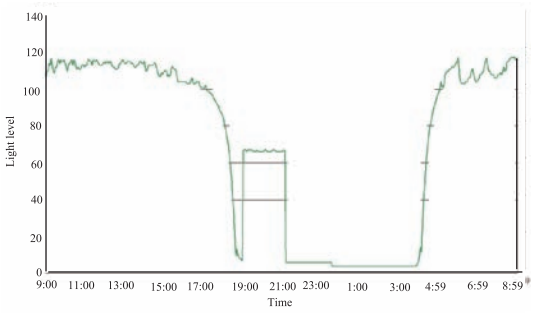

Fig. 12 Data synchronization test.

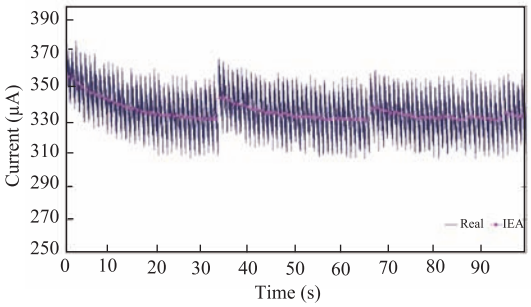

Fig. 13 Comparison of current measuring values.

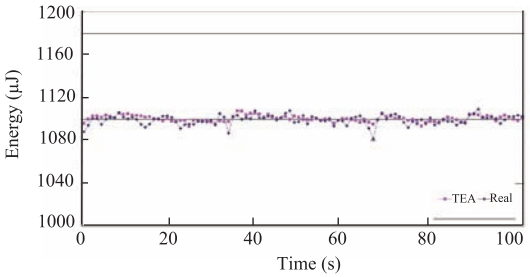

Fig. 14 Comparison of energy measurement values.

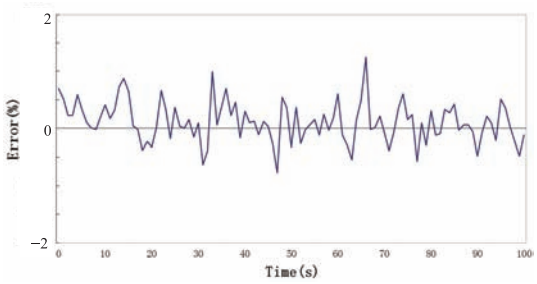

Fig. 15 Error of energy measurement.

is very close to the real value with an average error of −0.16%, and the standard deviation of error is 0.32%. Figure 14 compares the energy measured by IEA with that of the actual value. As shown in Fig. 15, the average error is 0.11% and the standard deviation of error is 0.35%. We can see that the energy measurement accuracy of IEA is high enough to support further network routing algorithm and promote the energy efficiency significantly. The power of the IEA energy measurement is approximately 157 μW, which can be further reduced by a low-power operational amplifier such as TSU104. The power of TSU104 may be less than 10 μW, but the measurement accuracy may decrease as well.

4.4 Experiment on energy prediction

In the experiment of energy prediction, we set the IEA node to sense the environmental data once per second and transmit the data every 10 s. The actual harvested energy is recorded by a multimeter and compared with the predicted

value. The results are shown in Fig. 16. After operating for 100 s continuously, the capacitance of capacitor C_1 calculated by IEA is 953.4 μF, which is 6.8 μF less than the actual value. The voltage of the solar panel is 5.71 V, and the internal resistance is 6357 Ω. In Fig. 16, the red line stands for real harvested energy, and the blue line indicates the harvesting energy per second in prediction. The average prediction error is -9.67%, and reasons affecting the accuracy are the following: First, due to the restriction of the multimeter, the measured real voltage value is not instantaneous value but average value per second, which affects the accuracy of real energy. Second, the energy measurement module consumes the energy when MCU is asleep, thereby leading to higher harvesting energy in actuality than that in prediction. The error can be reduced by adopting an amplifier with lower power. Third, the IEA node consumes less energy when not transferring data, so the voltage value varies minimally. Thus, the deviation of measurement and prediction of energy takes a larger proportion, leading to a relatively high error. We can observe that the accuracy of energy prediction is evidently higher when the IEA node is transmitting data. By the time of transmission and the following three seconds, the average error of prediction is 0.74% and the standard deviation for the error is 4.63%. In fact, the node requires exact prediction for energy when handling heavy tasks; when performing light tasks, the energy is relatively abundant and a lower accuracy of prediction can meet the requirement.

5 Conclusion

In this paper, we proposed a universal IEA EH-WSN platform, which provides an optimized energy management mechanism for intermittent operations. The IEA platform ensures that the network runs at a minimal level in an environment without energy harvesting, measures the energy with 99.89% accuracy, consumes only 157 μW of power, and provides strong support for EH-WSN. With regard to node performance and cost, the IEA platform adopts COT components. Thus, IEA is not only an experimental platform for EH-WSN, but is also an instrument with practical value.

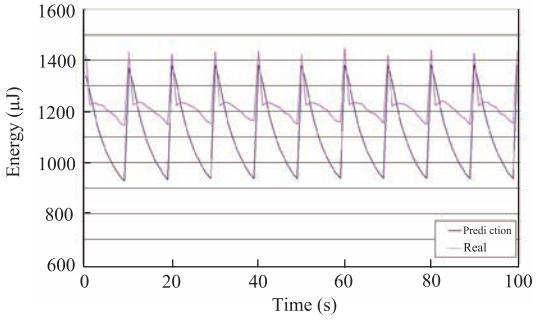

Fig. 16 Comparison of energy prediction values.

Acknowledgment

This work was supported in part by the Key Program of National Natural Science Foundation of China (No. 61632010), and Harbin Municipal Science and Technology Innovation Talent Research Funded Project (No. 2014RFQXJ027).

References

[1] Z. B. Zhou, W. Fang, J. W. Niu, L. Shu, and M. Mukherjee, Energy-efficient event determination in underwater WSNs leveraging practical data prediction, *IEEE Trans. Ind. Inf.*, vol. 13, no. 3, pp. 1238–1248, 2017.

[2] T. Shi, S. Y. Cheng, Z. P. Cai, Y. S. Li, and J. Z. Li, Exploring connected dominating sets in energy harvest networks, *IEEE/ACM Trans. Netw.*, vol. 25, no. 3, pp. 1803–1817, 2017.

[3] J. G. Yu, Y. Chen, L. R. Ma, B. G. Huang, and X. Z. Cheng, On connected target k-coverage in heterogeneous wireless sensor networks, *Sensors* (*Basel*), vol. 16, no. 1, p. E104, 2016.

[4] J. Li, S. Y. Cheng, Z. Cai, J. G. Yu, C. K. Wang, and Y. S. Li, Approximate holistic aggregation in wireless sensor networks, *ACM Trans. Sensor Netw.* (*TOSN*), vol. 13, no. 2, p. 11, 2017.

[5] C. Aranzazu-Suescun and M. Cardei, Distributed algorithms for event reporting in mobile-sink WSNs for internet of things, *Tsinghua Sci. Technol.*, vol. 22, no. 4, pp. 413–426, 2017.

[6] S. Y. Cheng, Z. P. Cai, J. Z. Li, and H. Gao, Extracting kernel dataset from big sensory data in wireless sensor networks, *IEEE Trans. Knowl. Data Eng.*, vol. 29, no. 4, pp. 813–827, 2017.

[7] T. Qiu, A. Y. Zhao, R. X. Ma, V. Chang, F. B. Liu, and Z. J. Fu, A task-efficient sink node based on embedded multi-core SoC for internet of things, *Future Generation Comput. Syst.*, vol. 82, pp. 656–666, 2018.

[8] X. Zheng, Z. P. Cai, J. Z. Li, and H. Gao, A study on application-aware scheduling in wireless networks, *IEEE Trans. Mob. Comput.*, vol. 16, no. 7, pp. 1787–1801, 2017.

[9] Z. B. Chen, A. F. Liu, Z. T. Li, Y. J. Choi, H. Sekiya, and J. Li, Energy-efficient broadcasting scheme for smart industrial wireless sensor networks, *Mobile Information Systems*, vol. 2017, p. 7538190, 2017.

[10] S. Y. Cheng, Z. P. Cai, and J. Z. Li, Curve query processing in wireless sensor networks, *IEEE Trans. Veh. Technol.*, vol. 64, no. 11, pp. 5198–5209, 2015.

[11] C. Park and P. H. Chou, AmbiMax: Autonomous energy harvesting platform for multi-supply wireless sensor

nodes, in *Proc. 3rd Ann. IEEE Communications Society on Sensor and Ad Hoc Communications and Networks*, Reston, VA, USA, 2007, pp. 168–177.

[12] M. Gorlatova, R. Margolies, J. Sarik, G. Stanje, J. X. Zhu, B. Vigraham, M. Szczodrak, L. Carloni, P. Kinget, I. Kymissis, et al., Prototyping energy harvesting active networked tags (EnHANTs), in *Proc. IEEE INFOCOM*, Turin, Italy, 2013, pp. 585–589.

[13] M. Buettner, B. Greenstein, and D. Wetherall, Dewdrop: An energy-aware runtime for computational RFID, in *Proc. 8th Usenix Conf. Networked Systems Design and Implementation*, Boston, MA, USA, 2011, pp. 197–210.

[14] L. Feng, J. G. Guo, F. Zhao, and H. L. Jiang, A novel analysis of delay and power consumption for polling schemes in the IoT, *Tsinghua Sci. Technol.*, vol. 22, no. 4, pp. 368–378, 2017.

[15] Z. B. Chen, A. F. Liu, Z. T. Li, Y. J. Choi, and J. Li, Distributed duty cycle control for delay improvement in wireless sensor networks, *Peer-to-Peer Netw. Appl.*, vol. 10, no. 3, pp. 559–578, 2017.

[16] T. Qiu, R. X. Qiao, and D. O. Wu, EABS: An event-aware backpressure scheduling scheme for emergency internet of things, *IEEE Trans. Mob. Comput.*, vol. 17, no. 1, pp. 72–84, 2018.

[17] A. F. Liu, Q. Zhang, Z. T. Li, Y. J. Choi, L. Jie, and N. Komuro, A green and reliable communication modeling for industrial internet of things, *Comput. Electr. Eng.*, vol. 58, pp. 364–381, 2017.

[18] T. Shi, S. Y. Cheng, Z. P. Cai, and J. Z. Li, Adaptive connected dominating set discovering algorithm in energy-harvest sensor networks, in *Proc. 35th Ann. IEEE Int. Conf. Computer Communications*, San Francisco, CA, USA, 2016, pp. 1–9.

[19] C. M. Vigorito, D. Ganesan, and A. G. Barto, Adaptive control of duty cycling in energy-harvesting wireless sensor networks, in *Proc. 4th Ann. IEEE Communications Society Conf. Sensor, Mesh and Ad Hoc Communications and Networks*, San Diego, CA, USA, 2007, pp. 21–30.

[20] X. J. Ren and W. F. Liang, Delay-tolerant data gathering in energy harvesting sensor networks with a mobile sink, in *Proc. 2012 IEEE Global Communications Conf.*, Anaheim, CA, USA, 2013, pp. 93–99.

[21] X. L. Wang, J. Gong, C. S. Hu, S. Zhou, and Z. S. Niu, Optimal power allocation on discrete energy harvesting model, *EURASIP J. Wireless Commun. Netw.*, vol. 2015, no. 1, p. 48, 2015.

[22] K. Nakayama, N. Dang, L. Bic, M. Dillencourt, E. Bozorgzadeh, and N. Venkatasubramanian, Distributed flow optimization control for energy-harvesting wireless sensor networks, in *Proc. 2014 IEEE Int. Conf. Communications*, Sydney, Australia, 2014, pp. 4083–4088.

[23] X. J. Ren, W. F. Liang, and W. Z. Xu, Quality-aware target coverage in energy harvesting sensor networks, *IEEE Trans. Emerg. Top. Comput.*, vol. 3, no. 1, pp. 8–21, 2015.

[24] J. R. Smith, A. P. Sample, P. S. Powledge, S. Roy, and A. Mamishev, A wirelessly-powered platform for sensing and computation, in *Proc. 8th Int. Conf. Ubiquitous Computing*, Orange County, CA, USA, 2006, pp. 495–506.

[25] M. Hassanalieragh, T. Soyata, A. Nadeau, and G. Sharma, UR-SolarCap: An open source intelligent auto-wakeup solar energy harvesting system for supercapacitor-based energy buffering, *IEEE Access*, vol. 4, pp. 542–557, 2016.

[26] S. Y. Cheng, J. Z. Li, and L. Yu, Location aware peak value queries in sensor networks, in *Proc. 2012 IEEE INFOCOM*, 2012, pp. 486–494.

[27] S. Y. Cheng, Z. P. Cai, J. Z. Li, and X. L. Fang, Drawing dominant dataset from big sensory data in wireless sensor networks, in *Proc. 2015 IEEE Conf. Computer Communications*, Hong Kong, China, 2015, pp. 531–539.

[28] J. Z. Li, S. Y. Cheng, H. Gao, and Z. P. Cai, Approximate physical world reconstruction algorithms in sensor networks, *IEEE Trans. Parallel Distrib. Syst.*, vol. 25, no. 12, pp. 3099–3110, 2014.

[29] R. Shigeta, T. Sasaki, D. M. Quan, Y. Kawahara, R. J. Vyas, M. M. Tentzeris, and T. Asami, Ambient RF energy harvesting sensor device with capacitor-leakage-aware duty cycle control, *IEEE Sens. J.*, vol. 13, no. 8, pp. 2973–2983, 2013.

[30] Y. Zhang, H. Gao, S. Y. Cheng, Z. P. Cai, and J. Z. Li, IEA: An intermittent energy aware platform for ultra-low powered energy harvesting WSN, in *Proc. 12th Int. Conf. Wireless Algorithms, Systems, and Appl.*, 2017, pp. 185–197.

[31] D. H. Jung, K. Kim, and S. O. Jung, Thermal and solar energy harvesting boost converter with time-multiplexing MPPT algorithm, *IEICE Electron. Express*, vol. 13, no. 12, p. 20160287, 2016.

Hong Gao received the BS degree in computer science from Heilongjiang University, China in 1988, the MS degree in computer science from Harbin Engineering University, China in 1991 and the PhD degree in computer science from the Harbin Institute of Technology, China in 2004 She is currently a professor in the School of Computer Science and Technology, Harbin Institute of Technology, China and she is a senior member of CCF. Her research interests include graph data management, sensor networks, and massive data management.

Siyao Cheng received the BS, MS, and PhD degrees in computer science from the Harbin Institute of Technology, in 2005, 2007, and 2012, respectively. She is an associate professor in the School of Computer Science and Technology, Harbin Institute of Technology, China. She worked as a postdoctoral scholar with Georgia State University from 2013 to 2014. Her research interests include big sensory data management and wireless sensor networks.

Yang Zhang received the BS and MS degrees from Heilongjiang University, China in 2004 and 2010, respectively. He is currently working toward the PhD degree in the School of Computer Science and Technology, Harbin Institute of Technology, China. His research areas focus on wireless sensor networks.

Jianzhong Li is a professor in the School of Computer Science and Technology, Harbin Institute of Technology, China. He was a visiting scholar with the University of California, Berkeley from 1985 to 1988, a staff scientist in the Information Research Group, Lawrence Berkeley National Laboratory, and a visiting professor with the University of Minnesota from 1998 to 1999. His research interests include data management systems, sensor networks, and data intensive computing.